Animal Nutrition 17 (2024) 11–24

Contents lists available at ScienceDirect

Animal Nutrition

journal homepage: http://www.keaipublishing.com/en/journals/aninu/

Original Research Article

The AMPK and AKT/GSK3β pathways are involved in recombinant proteins fibroblast growth factor 1 (rFGF1 and rFGF1a) improving glycolipid metabolism in rainbow trout (*Oncorhynchus mykiss*) fed a high carbohydrate diet

Huixia Yu [a], Shuo Geng [a], Shuai Li [a], Yingwei Wang [a], Xin Ren [b], Debin Zhong [a], Haolin Mo [a], Mingxing Yao [a], Jiajia Yu [a], Yang Li [a], Lixin Wang [a, *]

[a] College of Animal Science and Technology, Northwest A&F University, Yangling, Shaanxi 712100, China
[b] Meixian Aquaculture Farm of Shitouhe Reservoir Administration, Xianyang, Shaanxi 712000, China

ARTICLE INFO

Article history:
Received 13 May 2023
Received in revised form
30 September 2023
Accepted 15 October 2023
Available online 3 January 2024

Keywords:
Rainbow trout
Recombinant proteins
Fibroblast growth factor 1
Glycogen synthesis
Lipid deposition

ABSTRACT

Fibroblast growth factor 1 (FGF1) regulates vertebrate cell growth, proliferation and differentiation, and energy metabolism. In this study, we cloned rainbow trout (*Oncorhynchus mykiss*) *fgf1* and *fgf1a*, prepared their recombinant proteins (rFGF1 and rFGF1a), and described the molecular mechanisms by which they improve glycolipid metabolism in carnivorous fish. A 31-d feeding trial was conducted to investigate whether they could enhance glycolipid metabolism in rainbow trout on high-carbohydrate diets (HCD). A total of 720 rainbow trout (8.9 ± 0.5 g) were equally divided into 4 groups: the chow diet (CD) group injected with PBS, the HCD group injected with PBS, the HCD group injected with rFGF1 (400 ng/g body weight), and the HCD group injected with rFGF1a (400 ng/g body weight). The results showed that short-term HCD had a significant positive effect on the specific growth rate (SGR) of rainbow trout ($P < 0.05$). However, it led to an increase in crude fat, serum triglyceride (TG) and glucose content, as well as serum glutamic pyruvic transaminase (GPT) and glutamic oxalacetic transaminase (GOT) contents ($P < 0.05$), suggesting a negative health effect of HCD. Nevertheless, rFGF1 and rFGF1a showed beneficial therapeutic effects. They significantly reduced the crude fat content of the liver, serum TG, GOT, and GPT contents caused by HCD ($P < 0.05$). The upregulation in *atgl*, *hsl*, and *acc2* mRNAs implied the promotion of TG catabolism. Moreover, rFGF1 and rFGF1a contributed to promoting lipolysis by activating the AMPK pathway and reducing lipid accumulation in the liver caused by HCD. In addition, the rFGF1 and rFGF1a-treated groups significantly reduced serum glucose levels and elevated hepatic glycogen content under HCD, and increased glucose uptake by hepatocytes. We observed a decrease in mRNA levels for *pepck*, *g6pase*, and *pygl*, along with an increase in mRNA levels for *gys*, *glut2*, and *gk* in the liver. Furthermore, these proteins regulated hepatic gluconeogenesis and glycogen synthesis by increasing the phosphorylation level of AKT, ultimately leading to an increase in GSK3β phosphorylation. In conclusion, this study demonstrates that rFGF1 and rFGF1a can enhance lipolysis and glucose utilization in rainbow trout by activating the AMPK pathway and AKT/GSK3β axis.
© 2024 The Authors. Publishing services by Elsevier B.V. on behalf of KeAi Communications Co. Ltd. This is an open access article under the CC BY-NC-ND license (http://creativecommons.org/licenses/by-nc-nd/4.0/).

1. Introduction

Carbohydrates are the primary energy source for living organisms, and their wide availability makes them an indispensable component of commercial compound fish feeds: cost savings, reduction of protein consumption, ammonia emissions, and contamination of farm waters are among the benefits (Kamalam et al., 2017; Wen et al., 2022). Fish, particularly carnivorous ones,

* Corresponding author.
E-mail address: fisherwanglx@nwsuaf.edu.cn (L. Wang).
Peer review under responsibility of Chinese Association of Animal Science and Veterinary Medicine.

Production and Hosting by Elsevier on behalf of KeAi

https://doi.org/10.1016/j.aninu.2023.10.009
2405-6545/© 2024 The Authors. Publishing services by Elsevier B.V. on behalf of KeAi Communications Co. Ltd. This is an open access article under the CC BY-NC-ND license (http://creativecommons.org/licenses/by-nc-nd/4.0/).

have a lower capacity to utilize carbohydrates in comparison to mammals. When digestible carbohydrate levels exceed 20% to 30% of the diet, these fish suffer from prolonged postprandial glycemia (Kamalam et al., 2017; Steinberg et al., 2022) and growth impairment (Volkoff and London, 2018). As a result, the study of glucose metabolic homeostasis and utilization mechanisms in fish, particularly carnivorous fish, has received considerable attention.

Fibroblast growth factor 1 (FGF1) is a member of the 23-member fibroblast growth factor (FGF) family, also known as an acidic fibroblast growth factor. Interestingly, FGF1 is the only peptide in its family that binds to all four receptors of FGFR1–4 and thereby mediates their cellular responses. FGF1/FGFR1 signaling is involved in various signaling regimes, such as mammalian energy metabolism and growth (Gasser et al., 2017, 2022; Wang et al., 2023). Reportedly, FGF1 reduced plasma glucose levels in diabetic mice (Gasser et al., 2022; Xu et al., 2020), and FGF1 gene-deficient mice fed with a high-energy diet exhibited insulin resistance (Gasser et al., 2017; Jonker et al., 2012). Furthermore, intraventricular injection of FGF1 normalized blood glucose levels for up to 18 weeks, indicating a central role of FGF1 (Scarlett et al., 2016, 2019).

In addition to its potent hypoglycemic effect, peripheral injection of FGF1 also lessens obesity-associated hepatic steatosis and inflammation (Huang et al., 2017; Liu et al., 2016; Wang et al., 2023). In obese (ob/ob) mice, FGF1 reduced steatosis, suggesting a role for FGF1 in stimulating fatty acid oxidation or very low density lipoprotein (VLDL) secretion (Liu et al., 2016). Moreover, peroxisome proliferator-activated receptor γ (PPARγ) regulates FGF1 expression in adipose tissue strongly induced during a high-fat diet (Choi et al., 2016; Jonker et al., 2012). Notably, the results demonstrated that FGF1 inhibits the lipolytic effect of adipose tissue, which in turn inhibits hepatic gluconeogenesis to link glycolipid metabolism (Sancar et al., 2022).

Mammals and toads have one copy of the *fgf1* gene, and a few experiments indicated that cyprinids may have duplicate genes: FGF1a and FGF1b. Furthermore, FGF1a and FGF1b′s role in the growth and development of grass carp was reported and confirmed by zebrafish and mirror carp studies (Guo et al., 2017; Ma et al., 2014; Songhet et al., 2007). However, research on FGF1 in other fish has yet to be published. Rainbow trout (*Oncorhynchus mykiss*) is one of the most commonly farmed species in the world. Nevertheless, as a typical representative of "glucose intolerant" fish, the regulatory mechanism of its glucose metabolism remains poorly understood. This study aimed to achieve three objectives. First, we intended to clone the FGF1 and FGF1a of rainbow trout, prepare recombinant proteins, and examine their protective effects on rainbow trout under glucose stress. Second, we expected to evaluate the regulation of FGF1 on glycolipid metabolism in rainbow trout under high carbohydrate feeding profiles. Finally, we investigated the possible mechanisms and signaling pathways by which FGF1 exerts its regulatory effects on glycolipid metabolism.

2. Materials and methods

2.1. Animal ethics statement

All experiments were carried out in accordance with the "Guidelines for the Care and Use of Laboratory Animals" formulated by the Ministry of Science and Technology of China. The Northwest A&F University College Animal Welfare and Policy Committee approved this experiment under contract (NWAFU-314020038).

2.2. Molecular cloning and bioinformatics analysis of rainbow trout FGF1 and FGF1a

The primers for the test were designed based on the relevant sequence information of rainbow trout in the NCBI database (https://www.ncbi.nlm.nih.gov/). The primers (Table 1) were purchased from Sangong Biotechnology (Shanghai, China). Polymerase chain reaction (PCR) was performed to clone rainbow trout *fgf1* and *fgf1a*. The quality of the amplified products was assessed via 1% agarose gel electrophoresis, and the amplified products were subjected to DNA purification and recovery (Tiangen, Beijing, China). The DNA recovery products were attached to the pGEM-T Easy vector (Madison, WI, USA) and converted into a strain of *Escherichia coli* DH5α for random monoclonal sequencing. Multiple alignments of amino acid sequences of different species of FGF1 and FGF1a and the calculation of the similarity of amino acid sequences were realized by MEGA-X software (Pennsylvania State University, USA). Furthermore, the phylogenetic tree was constructed using the neighbor-joining (NJ) method, and bootstrap replication ($N = 1000$) was employed for testing.

2.3. Prokaryotic expression, purification and Western blotting detection of recombinant proteins

We prepared rFGF1 and rFGF1a proteins using the *E. coli* expression system. Based on the cloned rainbow trout *fgf1* and *fgf1a* cDNA sequences, the coding regions of these genes were subcloned into the pET-32a vector by PCR and double digestion. The restriction enzymes used by *fgf1* and *fgf1a* were 5′-BamHI/SalI-3′ and 5′-BamHI/XhoI-3′, respectively, with the introduction of 6 × His tag at the N-terminus. The sequenced recombinant plasmids pET32a/FGF1 and pET32a/FGF1a were converted into *E. coli* BL21 (DE3), and positive clones were selected with LB-ampicillin plates, followed by monoclonal culture in LB (ampicillin-resistant) medium. And at

Table 1
Primers used in this study.

Primer name	Sequences (5′-3′)	Purpose
fgf1	F: ATGGATCTGGTGACGCTGGGCT	Molecular cloning
	R: GTTGACAACACCACCATGTAA	
fgf1a	F; ATGACGGATGCAGAAATAACGT	
	R: TTGGAGGGCACAGGGAGTGA	
Beta-actin	F: GAAATCGCCGCACTGGTT	Reference gene
	R: CTCTTGCTCTGAGCCTCGTCT	
gapdh	F: TGACATCCCATGGGGAAACG	
	R: GTACCCGTCCTCGTTGACTC	
Q-pepck	F: CCCCTTCTTCGGCTACAACT	Real-time PCR
	R: GGCGTTGTCACCGAAACCC	
Q-g6pase	F: CTAGGCGTGGACCTGCTATG	
	R: GTCCTAAAGAGGGTCGTGCC	
Q-gk	F: AGATGACTGTGGGCATCGAC	
	R: GATGTCACAGTGAGGCGTCA	
Q-gys	F: GACAGAGAGGCCAACGACTC	
	R: ACTCATGGAAATGGGCGAGG	
Q-pygl	F: CACCTGGACGGGATTAGAGC	
	R: TCGCTGAAGTCTCGGAACAC	
Q-glut2	F: GAACGGTACAGGGACAGAGAA	
	R: AAGCCCACCAGGAAGGATGA	
Q-atgl	F: GCTGCAGAGTGTTCTTTCGC	
	R: GGGAGTGTTGCAATTCCAGC	
Q-hsl	F: AGGGTCATGGTCATCGTCTC	
	R: CTTGACGGAGGGACAGCTAC	
Q-fas	F: GAGACCTAGTGGAGGCTGTC	
	R: TCTTGTTGATGGTGAGCTGT	
Q-acc1	F: TGACAACATTGACGGACCCC	
	R: TGGCAATGAGGACCTTCTCG	
Q-acc2	F: CAGCTTGGTAAACAGCCTGG	
	R: TCCGCACATTCTTCCAGTCC	

fgf1 = fibroblast growth factor 1; *gapdh* = glyceraldehyde-3-phosphate dehydrogenase; *pepck* = phosphoenolpyruvate carboxykinase; *g6pase* = glucose-6-phosphatase; *gk* = glucose kinase; *gys* = glycogen synthase; *pygl* = glycogen phosphorylase; *glut2* = glucose transporter 2; *atgl* = adipose triglyceride lipase; *hsl* = hormone-sensitive lipase; *fas* = fatty acid synthase; *acc* = acetyl-CoA carboxylase.

OD_{600} value of 0.6, isopropyl-β-D-thiogalactopyranoside (IPTG, 0.8 mmol/L) was added with induction overnight at 27 °C (180 rpm/min). Inclusion bodies were sonicated, dissolved in 8 mol/L urea, and washed with Ni-NTA His-Bind resin. Purified rFGF1 and rFGF1a proteins were dialyzed against gradient Tris–HCl buffers containing different concentrations of urea until urea was removed from rFGF1 and rFGF1a proteins. The protein concentration was determined using the BCA protein concentration kit (Biosharp, Beijing, China), and rFGF1 and rFGF1a were detected using SDS-PAGE electrophoresis. After electrophoresis, the gel was stained with Komas Brilliant Blue R-250 for 60 min and then destained until protein bands were visible.

The Western blotting technique was employed to detect the His-tagged recombinant proteins obtained. The experimental procedure for this technique was as follows: protein samples were separated by SDS-PAGE, transferred to PVDF membranes (0.22 μm), placed on a shaker for 1.5 h, and incubated overnight at 4 °C with various targeting antibodies (Table 2). The next day, the enzyme-labeled secondary antibody was incubated at room temperature for 1 h, washed with TBST, and protected from light. The membranes were washed again and developed using the ECL detection kit (Solarbio, Beijing, China) and the chemiluminescence detection system (Bio-Rad, California, USA).

2.4. Experimental fish, diets, and experimental design

Rainbow trout were obtained from the Stone River Aquaculture Farm (Meixian, Shaanxi, China). Feed formulation and proximate composition utilized in this study are provided in Table 3. After preparation, the diets were dried and stored at −20 °C until use. Prior to the experiment, the fish were temporarily reared in the flow-through culture pond for 2 weeks. At the end of the temporary culture, juvenile rainbow trout of normal size and vigor (8.9 ± 0.5 g) were randomly assigned to the flow-through culture pond for the test. The size of each breeding pool was 2 m × 1.2 m × 0.8 m, and the water flow was 50 L/h. The daily feeding was approximately 4% of body weight. Rainbow trout were weighed every 7 d using a small scale and the feeding rate was adjusted. Feed residue remaining after 1 h of feeding was aspirated, dried, and weighed to determine feed intake (FI). Fish were weighed once a week and the daily feeding amount adjusted. Water temperature (16 to 18 °C), pH (7.0 to 7.4), dissolved oxygen (>7 mg/L), and ammonia nitrogen (<0.0075 mg/L) were maintained during feeding. The experimental design was as follows.

Experiment 1: We injected juvenile rainbow trout with various concentrations of the recombinant proteins to determine whether the rFGF1 and rFGF1a proteins were biologically active and the optimal dose to produce an effect. The experiment included 9 groups of 6 fish, each with 3 replicates. The groups were divided based on the type and dosage of injection administered, which included PBS injection, rFGF1 injection (at 200, 400, 800, and 1600 ng/g body weight), and rFGF1a injection (at 200, 400, 800, and 1600 ng/g body weight). Samples were collected 2 h following the injection.

Experiment 2: We performed a glucose stress test on rainbow trout to determine the effect of rFGF1 and rFGF1a proteins, and the injection dose was determined by the results of experiment 1. Fish were categorized into 4 groups (PBS injection, glucose injection (250 mg/kg), glucose + rFGF1, and glucose + rFGF1a groups) with 6 fish in each group and 3 replicates at the end of the transient period. Serum and tissue samples were collected 2 and 6 h after injection, respectively. Samples were collected from the 0 h post-injection and un-injected groups to control for the potential effects of the physical injection.

Experiment 3: A 31-d culture experiment was carried out to investigate the therapeutic effects of rFGF1 and rFGF1a on rainbow trout. At the end of the acclimatization period, the fish were divided into 4 groups of 60 fish with 3 replicates. One group received a chow diet (CD), while the other 3 groups were provided with a high-carbohydrate diet (HCD). Weekly, 6 samples from both the CD and HCD groups were randomly collected and analyzed for serological indicators. At the end of the third week, fish in the CD group were injected with PBS, and fish in HCD groups were injected with PBS, rFGF1, and rFGF1a, respectively. The injection dose was determined based on the findings of experiment 1. Subsequently, samples were collected in 3, 7, and 10 d post-injection.

Table 2
Antibodies used for Western blotting assay.

Antibodies name	Source	Identifier
AKT	Cell signaling technology (Boston, USA)	Cat #4691
p-AKT (Ser473)	Cell signaling technology (Boston, USA)	Cat #4060
GSK3β	Abways (Shanghai, China)	AB3168
p-GSK3β (Ser9)	Abways (Shanghai, China)	CY6248
Beta-actin	Abmart (Shanghai, China)	PHE7207
His-tag	Abmart (Shanghai, China)	M30111
Goat anti-mouse IgG-HRP	Abmart (Shanghai, China)	M21001
Goat anti-rabbit IgG-HRP	Abmart (Shanghai, China)	M21002

AKT = serine/threonine kinase; GSK3β = glycogen synthase kinase 3β.

Table 3
Diet formulation and proximate composition of each group (g/kg, dry-matter basis).

Item	Treatment	
	CD	HCD
Ingredients		
Fish meal	350	350
Casein	180	180
Soybean meal	80	80
Corn starch	100	240
Soybean oil	100	100
$Ca(H_2PO_4)_2$	20	20
Bentonite	80	10
Microcrystalline cellulose	80	10
Vitamin-mineral premix[1]	10	10
Proximate composition[2]		
Moisture	88	90
Crude protein	418	410
Crude lipid	121	129
Ash	143	82

CD = chow diet; HCD = high-carbohydrate diet.
[1] The vitamin-mineral premix contains (mg or IU per kilogram of diet): vitamin A, 6000 IU; vitamin D, 2000 IU; vitamin E, 80 IU; vitamin C, 200 mg; niacin, 100 mg; pantothenic acid, 35 mg; folic acid, 10 mg; thiamine, 15 mg; riboflavin, 15 mg; pyridoxine HCl, 12 mg; cyanocobalamin, 0.03 mg; menadione, 20 mg; inositol, 200 mg; folic acid, 6 mg; biotin, 0.5 mg; Fe, 130 mg; Mg, 110 mg; Co, 0.4 mg; Zn, 70 mg; Se, 0.5 mg; Cu, 4 mg; I, 0.8 mg; Mn, 20 mg.
[2] Values are reported as the mean values of duplicate analyses.

2.5. Sample collection

Feeding tests required fasting for 24 h before sampling. Fish were caught randomly and anesthetized with tricaine methanesulfonate (MS-222). Body and liver weights were measured individually, and serum samples were collected and stored temporarily at 4 °C for 3 h, followed by brief centrifugation (1000 × *g*) at 4 °C to obtain serum, which was later stored at −80 °C. Liver samples were snap-frozen in liquid nitrogen immediately after obtaining them. The livers and whole fish were stored at −20 °C for proximate compositional analysis. Additionally, liver samples were collected and fixed in 4% paraformaldehyde for histological analysis.

2.6. Growth performance

Individual fish were weighed and their data were collected. Growth performance, survival rate (SR), and hepatosomatic index (HSI) were calculated using data on fish weight, number and the weight of organs with the following equations:

Weight gain rate (WGR, %) = [(final weight, g) − (initial weight, g)] / (initial weight, g) × 100;

SR (%) = final fish number/initial fish number × 100;

FI (g/g per day) = 100 × {amount of FI/[(final weight + initial weight)/2]}/number of days;

Specific growth rate (SGR, %/d) = [ln (final weight, g) − ln (initial weight, g)]/number of days reared × 100;

HSI (%) = (liver weight, g)/ (individual fish weight, g) × 100.

2.7. Biochemical parameter analysis

To determine the moisture, crude protein, crude lipid and ash contents of the diet samples and experimental fish, the AOAC official methods of analysis (AOAC, 2005) were used. Six juvenile rainbow trout were used for each body composition test. Briefly, the moisture content was measured by drying the samples in the oven at 105 °C to reach constant weight, crude protein content was determined using a Kjeltec Analyzer Unit (Kjeltec 8400, FOSS, Denmark), crude fat content was measured by the Soxhlet extraction method, and ash content was measured by incinerating the samples in a muffle furnace (BF51894C-1, Thermo Fisher Scientific, USA) at 550 °C until constant weight. Glucose, glycogen, glutamic oxaloacetic transaminase (GOT), glutamic pyruvic transaminase (GPT), and triglyceride (TG) were all tested using specific commercial assay kits. Except for the TG kit, which was from Beijing Pulilai Gene Technology, all were from Nanjing Jiancheng Institute of Biological Engineering (Nanjing, China). Commercial kits were used according to the manufacturer's instructions.

2.8. Total RNA extraction, cDNA synthesis and real-time quantitative PCR

Total RNA extractions were performed using the Trizol method. RNA sample quality was determined by agarose gel electrophoresis and a Nanodrop 2000 spectrophotometer (Thermo Fisher Scientific, USA). The cDNA was generated at the same concentration using a reverse transcription kit with real-time quantitative PCR (RT-qPCR). Rainbow trout β-actin and *gapdh* were used as reference genes. To ensure greater accuracy in our results, we set up 3 replicates for each PCR assay and calculated the data using the $2^{-\Delta\Delta Ct}$ method. This approach also took into account the specificity of the melting curve reaction amplification.

2.9. Histological analysis

Liver samples were fixed in 4% paraformaldehyde for 48 h, embedded in paraffin, and cut into 6-μm sections. Next, they were dewaxed using xylene and hydrated with different concentrations of alcohol to allow the dye to enter the tissue. Sections were stained with hematoxylin-eosin and sealed with neutral resin. Histological features were observed and photographed with an optical microscope (Nikon Ds-Ri2, Japan). Evaluation of liver features primarily involved observing and analyzing pathological characteristics such as liver vacuolization, lipid droplet count, and inflammatory cell infiltration in pathological sections (Fujisawa et al., 2021; Yu et al., 2021).

2.10. Isolation of primary hepatocytes and treatment with rFGF1 and rFGF1a

Three-day starved rainbow trout of approximately 50 g body weight were anesthetized using MS-222. Moreover, the livers were removed after tail vein blood sampling, temporarily stored in pre-cooled PBS buffer (containing penicillin and streptomycin) and brought into the cell chamber. Blood clots and connective tissues were carefully removed from an ultra-clean bench, cut into 1 mm^3 tissue pieces with scissors and washed several times in PBS. We used enzymatic digestion to isolate primary hepatocytes. Tissue blocks were digested in 0.5 g/L collagenase IV (Yuanye, Shanghai, China) PBS buffer for 30 min, sequentially filtered through 100- and 70-μm sieves, and centrifuged at 1000 × *g* at 4 °C for 4 min. Liver parenchymal cells were purified using a percoll separating solution (Solarbio, China). Finally, cell suspensions were made by adding DMEM medium (15% fetal bovine serum, and 1 × penicillin/streptomycin), stained with 0.4% trypan blue and counted and inoculated at appropriate density in 25 cm^2 cell culture flasks and incubated at 20 °C in a humidified incubator containing 5% CO_2.

Hepatocytes for the cytotoxicity assay were inoculated in 96-well cell plates and incubated with different concentrations of rFGF1 and rFGF1a proteins (0, 20, 50, 75, 100 ng/μL) for 24 h, cytotoxicity was detected using the Cell Counting Kit-8 (CCK8) assay (Promega, USA).

To verify the function of FGF1 and FGF1a at the cellular level, we inoculated primary hepatocytes at the peak growth stage on 6-well plates in 4 treatment groups and triplicate. They were LG group (1 g/L glucose), HG group (4.5 g/L glucose + 200 μM oleic acid), HG + rFGF1 group (4.5 g/L glucose + 200 μM oleic acid + 50 ng/μL rFGF1), HG + rFGF1a group (4.5 g/L glucose + 200 μM oleic acid + 50 ng/μL rFGF1a) treated cells for 24 h and a portion of the cells were used to collect test samples, including RNA samples, cell supernatants, and precipitates.

In addition, we performed a 2-Deoxy-2-[(7-nitro-2,1,3-benzoxadiazol-4-yl)amino]-D-glucose (2-NBDG) assay. The 2-NBDG is a fluorescent glucose analog for detecting glucose uptake in living cells. Briefly, we incubated differently treated cells with 2-NBDG for 1 h at 18 °C protected from light. Then, we examined the fluorescence intensity by fluorescence microscopy and checked the readings at 480/520 nm with a microplate reader.

2.11. Statistical analysis

Data were analyzed by one-way ANOVA. A *P*-value < 0.05 ($P < 0.05$) was considered statistically significant. All experimental values were expressed as mean ± standard error (SEM). All statistical analyses were performed using SPSS 20.0 software (IBM Corporation, Armonk, NY, USA) and GraphPad Prism 7.0 software (GraphPad Software, CA, USA) was employed for graphs.

3. Results

3.1. Identification of fgf1 and fgf1a cDNAs in rainbow trout

Cloned rainbow trout *fgf1* contains a 735 bp open reading frame (accession number: OQ710135) encoding 244 amino acids; rainbow trout *fgf1a* has a 480 bp open reading frame (accession number: OQ710136) encoding 159 amino acids (Fig. S1). An FGF structural domain confirmed that they were members of the FGF family

(Fig. 1A), and we searched for amino acid sites for their binding to heparin, shown in Fig. S1. The results of multiple alignments showed a low sequence identity (59.8%) between rainbow trout FGF1 and FGF1a. However, they showed a high sequence similarity with the direct homologs of FGF1 and FGF1a in teleosts (*Salmo salar* FGF1, 96%; *S. salar* FGF1a, 91.8%). Interestingly, their homology with mammals was lower (*Homo sapiens* FGF1, 57%; *H. sapiens* FGF1a, 50.9%). In addition, a phylogenetic tree was constructed using the amino acid sequences of FGF1 and FGF1a from different species. The results are shown in Fig. 1B, where rainbow trout FGF1 and FGF1a are nested into the branch of teleost, mammalian FGF1 and FGF1a are clustered into one group, and amphibians are also clustered together, showing their different evolutionary status.

3.2. Purification and Western blotting analysis of rFGF1 and rFGF1a

To investigate the biological functions of rainbow trout FGF1 and FGF1a, recombinant plasmids pET32a/FGF1 and pET32a/FGF1a were transformed into *E. coli* BL21 (DE3). Upon induction with IPTG, SDS-PAGE electrophoresis of the strains carrying these plasmids showed high expression levels (Fig. 2A and C). The rFGF1 and rFGF1a were approximately 45 and 36 kDa, respectively (theoretically, rFGF1 is 26.9 kDa, and rFGF1a is 17.6 kDa). The expected bands were visible after purification utilizing nickel columns for washing (Fig. 2B and D). We used anti-His-tagged mouse monoclonal antibodies to detect rFGF1 and rFGF1a in induced-expression reorganized proteins (Fig. 2E). Furthermore, we employed enterokinase

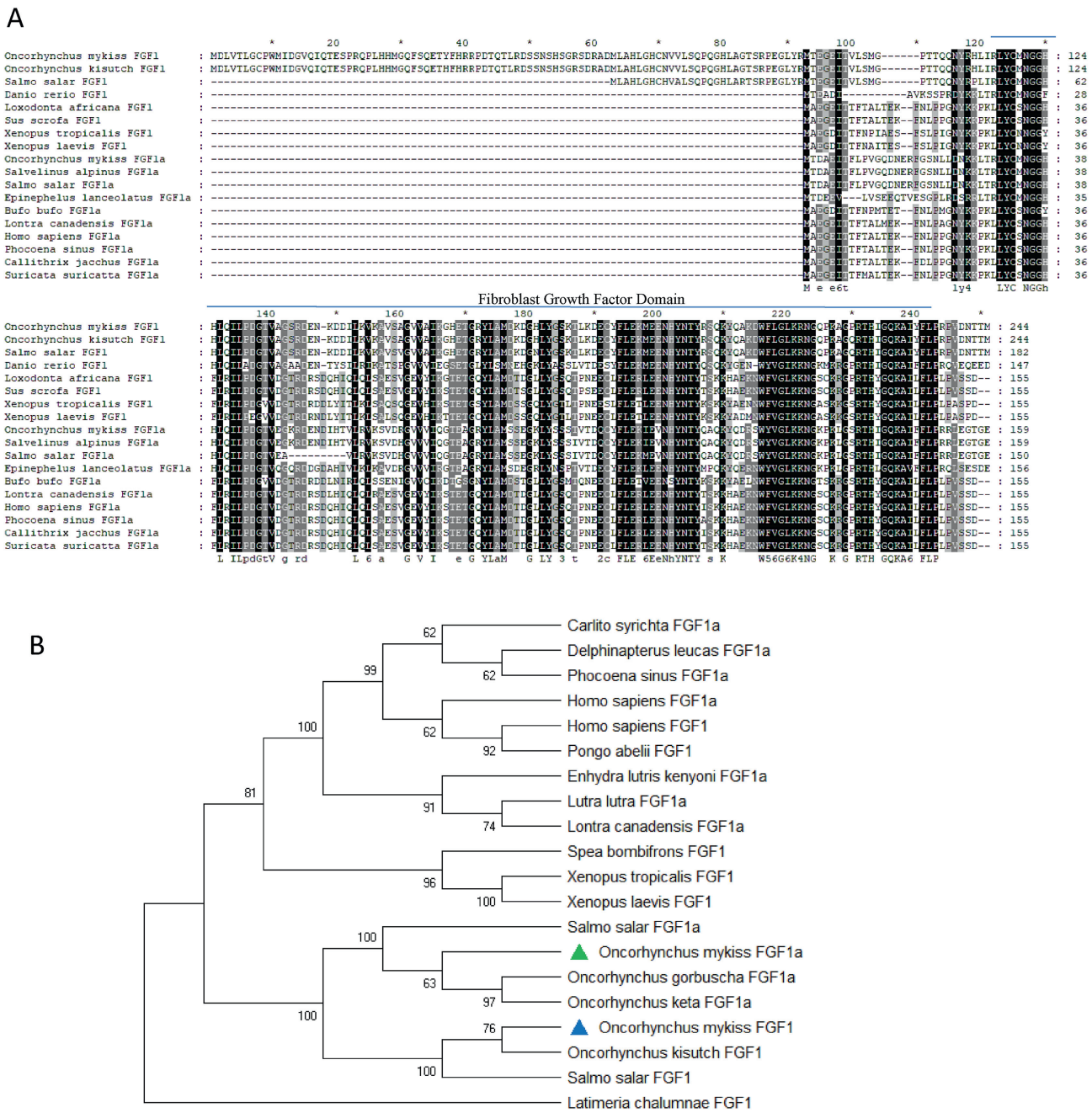

Fig. 1. Bioinformatics analysis of rainbow trout FGF1 and FGF1a. (A) Multiple sequence alignments of rainbow trout FGF1 and FGF1a with FGF1 and its isoforms from other vertebrates. (B) Phylogenetic relationships of FGF1 proteins in vertebrates. Target species are marked with blue and green triangles. The sequences utilized for both the multiple alignments and phylogenetic tree construction can be found in Table S1. FGF = fibroblast growth factor.

to cut and remove the His-tag and sulfur protein to prevent specific reactions between protein tags and proteins. Following protease cleavage, SDS-PAGE was used to reveal the true size of rFGF1 and rFGF1a (Fig. 2F).

To establish the appropriate dose for future experiments, we conducted a study on the impact of our homologous recombinant proteins on glucose metabolism genes in rainbow trout. This was achieved through an acute intraperitoneal injection. In our study, expression of phosphoenolpyruvate carboxykinase (*pepck*) and glucose-6-phosphatase (*g6pase*) genes, both of which are involved in gluconeogenesis, was significantly reduced. Additionally, we observed increased expression of the glycolytic gene glucose kinase (*gk*) following the injection of varying concentrations of recombinant proteins into juvenile fish. This effect was most pronounced at a concentration of 400 ng/g body weight (Fig. S2). As a result, we chose to use this concentration for all subsequent experiments.

3.3. Acute effects of rFGF1 and rFGF1a injections on rainbow trout under high glucose stress

Following 2 weeks of acclimation, rainbow trout were intraperitoneally injected with PBS, glucose, rFGF1, and rFGF1a, respectively. Samples were collected from the un-injected group and those groups injected with the substance at 0, 2, and 6 h intervals. The samples were analyzed to determine any changes in serum glucose levels, serum TG, and mRNA expression involved in glucose metabolism. The sample analysis of the un-injected group and the group injected at 0 h revealed no significant differences in the indicators (Fig. S3). The findings suggested that rFGF1 and rFGF1a led to a notable reduction in serum glucose levels 2 h post-injection compared to the group that received a glucose injection (Fig. 3A). However, there was no significant alteration in serum TG levels within the same 2-h timeframe (Fig. 3B). Furthermore, the mRNA levels of *pepck* and *g6pase* were significantly reduced. rFGF1a (but not rFGF1) was upregulated in the

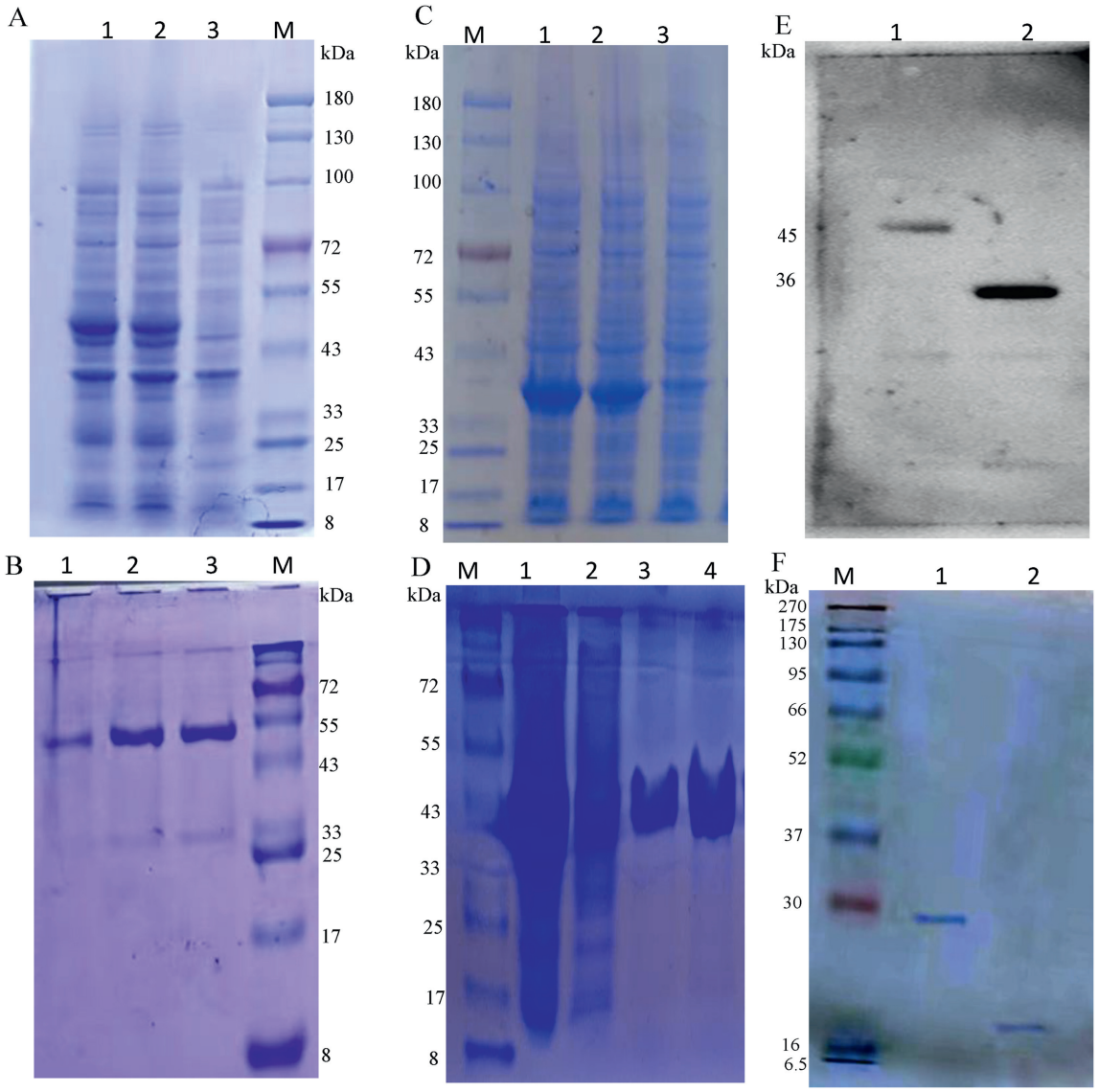

Fig. 2. SDS-PAGE and Western blotting analysis of rFGF1 and rFGF1a. The induced expression of (A) rFGF1 and (C) rFGF1a. Lanes 1 and 2, proteins expressed in *Escherichia coli* after IPTG induction; lane 3, *E. coli* before induction. Purified (B) rFGF1 and (D) rFGF1a proteins. (E) Western blotting analysis of rFGF1 and rFGF1a using anti-His tag antibody. (F) SDS-PAGE of rFGF1 and rFGF1a after enterokinase cleavage. Lanes 1 and 2 are FGF1 and FGF1a recombinant proteins, respectively. rFGF1 = recombinant protein fibroblast growth factor 1; rFGF1a = recombinant protein fibroblast growth factor 1a; IPTG = isopropyl-β-D-thiogalactopyranoside.

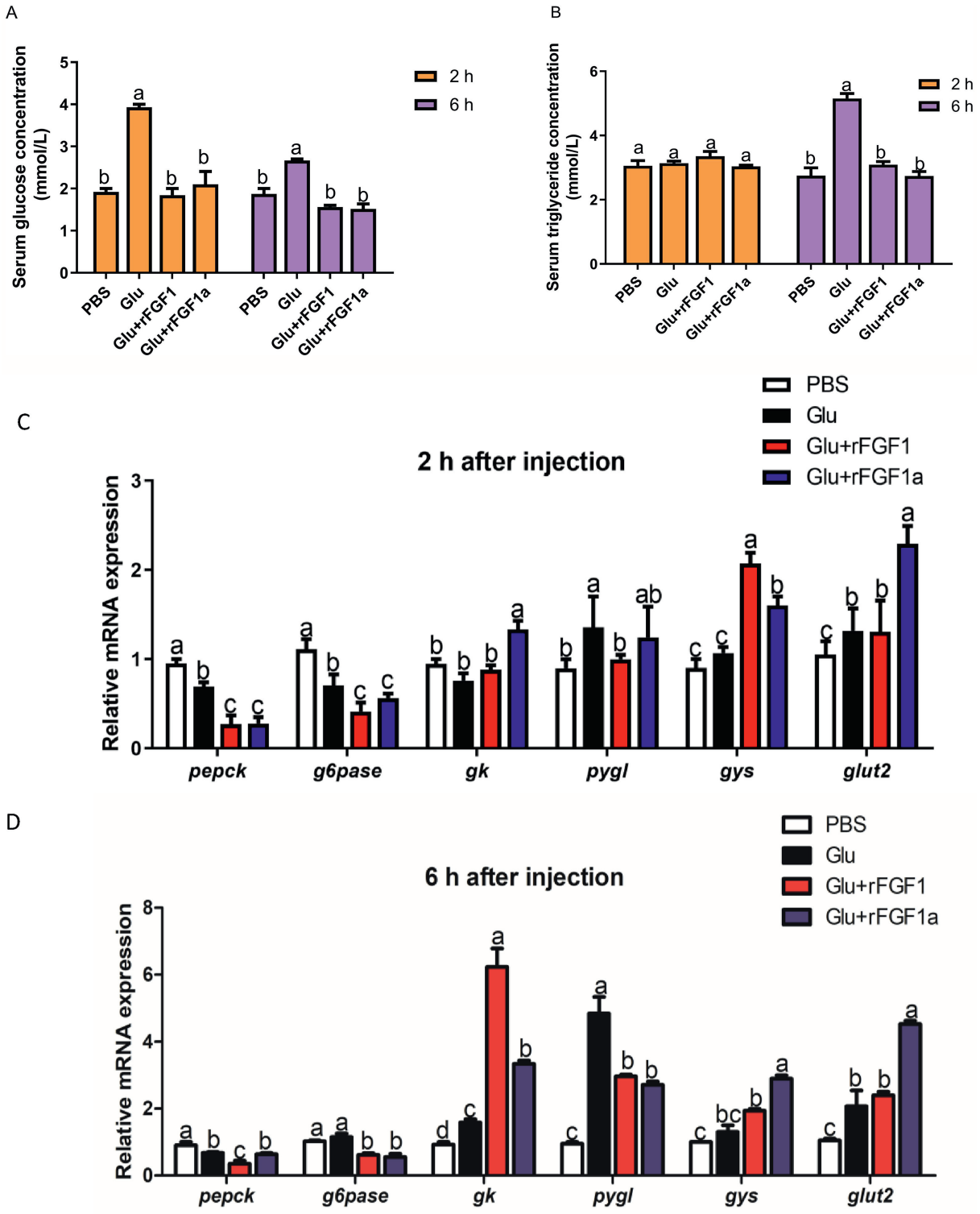

Fig. 3. Glucose stress test. (A) Effect of different treatments on serum glucose levels of rainbow trout. (B) Effect of different treatments on serum triglyceride levels in rainbow trout. (C and D) Expression abundance of glucose metabolism genes in the liver at different times. *pepck* = phosphoenolpyruvate carboxykinase; *g6pase* = glucose-6-phosphatase; *gk* = glucose kinase; *pygl* = glycogen phosphorylase; *gys* = glycogen synthase; *glut2* = glucose transporter 2. PBS = phosphate buffer saline; Glu = glucose (250 mg/kg); Glu + rFGF1 = glucose (250 mg/kg) + rFGF1 (400 ng/g body weight); Glu + rFGF1a = glucose (250 mg/kg) + rFGF1a (400 ng/g body weight). [a-d] Different letters indicate significant differences between groups ($P < 0.05$).

glycolytic gene *gk* at 2 h post-injection. Expression of the most important glucose transporter protein gene (glucose transporter 2 [*glut2*]) in the liver was increased in the other three groups compared with the PBS-injected group (Fig. 3C). Additionally, rFGF1 and rFGF1a expressed significant reductions in serum glucose levels and serum TG at 6 h after injection, compared with glucose injection groups (Fig. 3A and B). Concerning glucose metabolism, the genes *pepck* and *g6pase* remained low, while the *gk* involved in glycolysis was upregulated in Glu + rFGF1 and Glu + rFGF1a groups at 6 h post-injection, compared to glucose group. Additionally, a decrease in glycogen

Table 4
Effects of different treatments on the growth performance of rainbow trout juveniles.

Diet	Injection	FBW, g	SR, %	FI, g/g per day	WGR, %	SGR, %/d	HSI, %
CD	PBS	14.6 ± 1.1[b]	96.2 ± 2.1	2.0 ± 0.6	64.04 ± 4.55[b]	1.77 ± 0.01[b]	1.12 ± 0.04[c]
HCD	PBS	17.3 ± 0.9[a]	93.4 ± 2.7	1.6 ± 0.2	94.38 ± 1.62[a]	2.37 ± 0.02[a]	1.50 ± 0.03[a]
HCD	rFGF1	17.5 ± 1.1[a]	94.4 ± 2.2	1.6 ± 0.4	96.63 ± 2.32[a]	2.41 ± 0.01[a]	1.39 ± 0.07[b]
HCD	rFGF1a	16.8 ± 0.8[a]	92.6 ± 1.9	1.7 ± 0.3	88.76 ± 1.91[a]	2.27 ± 0.03[a]	1.34 ± 0.06[b]

IBW = initial body weight; FBW = final body weight; SR = survival rate; FI = food intake; WGR = weight gain rate; SGR = specific growth rate; HSI = hepatosomatic index; CD = chow diet; HCD = high-carbohydrate diet; rFGF1 = recombinant protein fibroblast growth factor 1; rFGF1a = recombinant protein fibroblast growth factor 1a.
[a–c] Within a column, means that are significantly different by Tukey's test are indicated by different letters ($P < 0.05$).

Table 5
Effects of different treatments on the body nutrient composition of juvenile rainbow trout (fresh weight, %).

Diet	Injection	Moisture	Crude protein	Crude ash	Crude fat
CD	PBS	72.9 ± 0.8	14.77 ± 0.03[b]	2.62 ± 0.10	83.1 ± 0.9[b]
HCD	PBS	72.1 ± 0.2	15.56 ± 0.05[ab]	3.03 ± 0.09	93.2 ± 0.6[a]
HCD	rFGF1	73.7 ± 0.4	17.11 ± 0.01[a]	2.81 ± 0.10	67.1 ± 1.2[c]
HCD	rFGF1a	72.0 ± 0.6	16.26 ± 0.05[a]	3.04 ± 0.06	73.3 ± 0.4[c]

CD = chow diet; HCD = high-carbohydrate diet; rFGF1 = recombinant protein fibroblast growth factor 1; rFGF1a = recombinant protein fibroblast growth factor 1a.
[a–c] Within a column, values with different superscripts are significantly different ($P < 0.05$).

phosphorylase (*pygl*) was observed along with an increase in glycogen synthase (*gys*) in rFGF1- and rFGF1a-injected groups, compared to glucose injection group. It is worth noting that the gene expression of *glut2* remained abundant during this time (Fig. 3D).

3.4. Growth performance and morphological indicators

Table 4 displays the results of several treatments on the growth performance of rainbow trout. The SR was greater than 92% ($P > 0.05$) for all groups during the feeding period. The average weight of fish in the HCD group was higher than CD group after feeding for 4 week. When rFGF1 and rFGF1a were administered with HCD, the final body weight (FBW), WGR, and SGR were not significantly different compared to the PBS-injected HCD group; the HSI was significantly lower than in the HCD group injected with PBS but higher than that of the CD group.

Table 5 showed the effect of several treatments on the body composition of rainbow trout. Moisture content and crude ash content did not vary significantly between treatments. The CD group contained slightly less crude protein than the HCD group ($P > 0.05$). The crude fat content of whole fish was greatly reduced after injection of recombinant proteins, and the crude fat in the CD group was much lower than that in the HCD group ($P < 0.05$).

3.5. Effect of rFGF1 and rFGF1a on lipid deposition

This study also examined lipid deposition-related factors (Fig. 4). The findings demonstrated that feeding HCD to rainbow trout dramatically increased the crude fat of whole fish (Fig. 4A), liver crude fat content (Fig. 4B), and serum TG levels (Fig. 4C). Additionally, the serum levels of GOT (Fig. 4D) and GPT (Fig. 4E) also increased. The injection of rFGF1 and rFGF1a affected the outcomes. Specifically, liver crude fat and whole-fish crude fat decreased 7 d after the injection (Fig. 4A and B).

We also gathered serological samples at various intervals following a single injection. During d 3 and 7 following injection of rFGF1 and rFGF1a, serum TG, GOT, and GPT levels were reduced when compared to the PBS-injection group. The results of d 10 for each group showed evidence of a rebound, although the treated group of rFGF1a remained inferior to the PBS group (Fig. 4C–E). In addition, we examined the histological characteristics (Fig. 4F) and observed a significant reduction in the number of vacuoles in the juvenile rainbow trout hepatocytes treated with rFGF1 and rFGF1a compared to those injected with PBS. It displayed the abundance of lipid metabolism-related gene expression for each treatment group (Fig. 4G). The HCD led to a decrease in the expression of lipolysis-related genes, specifically adipose triglyceride lipase (*atgl*), hormone-sensitive lipase (*hsl*), and acetyl-CoA carboxylase 2 (*acc2*). This trend was reversed by the exogenous administration of two recombinant proteins and reached a peak 3 d after injection. Moreover, rFGF1 and rFGF1a downregulated the lipid synthesis genes, fatty acid synthase (*fas*) and acetyl-CoA carboxylase 1 (*acc1*) on d 3 and 7 after injection. The Western blotting results indicated that injection of rFGF1 and rFGF1a led to a significant increase in the phosphorylation levels of adenosine monophosphate (AMP)-activated protein kinase (AMPK) in comparison to the PBS injection group ($P < 0.05$) (Fig. 4H).

3.6. Effect of rFGF1 and rFGF1a on glucose metabolism

Serum glucose levels and liver glycogen levels ($P < 0.05$) were significantly higher in rainbow trout fed an HCD (Fig. 5A and B). This effect was changed with exogenous delivery of the recombinant proteins (Fig. 5A). The rFGF1 demonstrated lower glucose levels on d 10 after injection, whereas rFGF1a displayed a lower temporal effect than rFGF1. For hepatic glycogen (Fig. 5B), the rFGF1 group had the highest glycogen content on d 7 and continued to have higher hepatic glycogen levels than the PBS-injected group on d 10. rFGF1a was slightly less time-sensitive than the rFGF1 group, although it had an earlier onset of action, showing an elevated hepatic glycogen trend at d 3. To investigate the role of rFGF1 and rFGF1a in regulating glucose metabolism in rainbow trout, we tracked hepatocyte glucose uptake using 2-NBDG (Fig. 5C). Cytotoxicity of different concentrations of recombinant protein on rainbow trout hepatic parenchymal cells is shown in Fig. S4. Compared to the treatment with a low glucose concentration, the fluorescence intensity of 2-NBDG was diminished in a culture environment high in glucose. The effects of high glucose on hepatocytes were counteracted and glucose uptake was reversed by rFGF1 and rFGF1a treatment (Fig. 5C). This result was consistent with the finding for the glucose content of the treated supernatants (Fig. 5D); the reduced glucose in the remaining supernatants corresponded to higher glucose uptake.

3.7. Effect of rFGF1 and rFGF1a on serine/threonine kinase (AKT)-glycogen synthase kinase 3β (GSK3β) axis and glucose metabolism-related gene expression

In the liver, glucose transport is mainly mediated by the *glut2*. Therefore, we assessed the expression of *glut2* mRNA by RT-qPCR. In rainbow trout fed on HCD, the expression of *glut2* was upregulated (Fig. 6A). Additionally, on d 3 post-injection, *glut2*

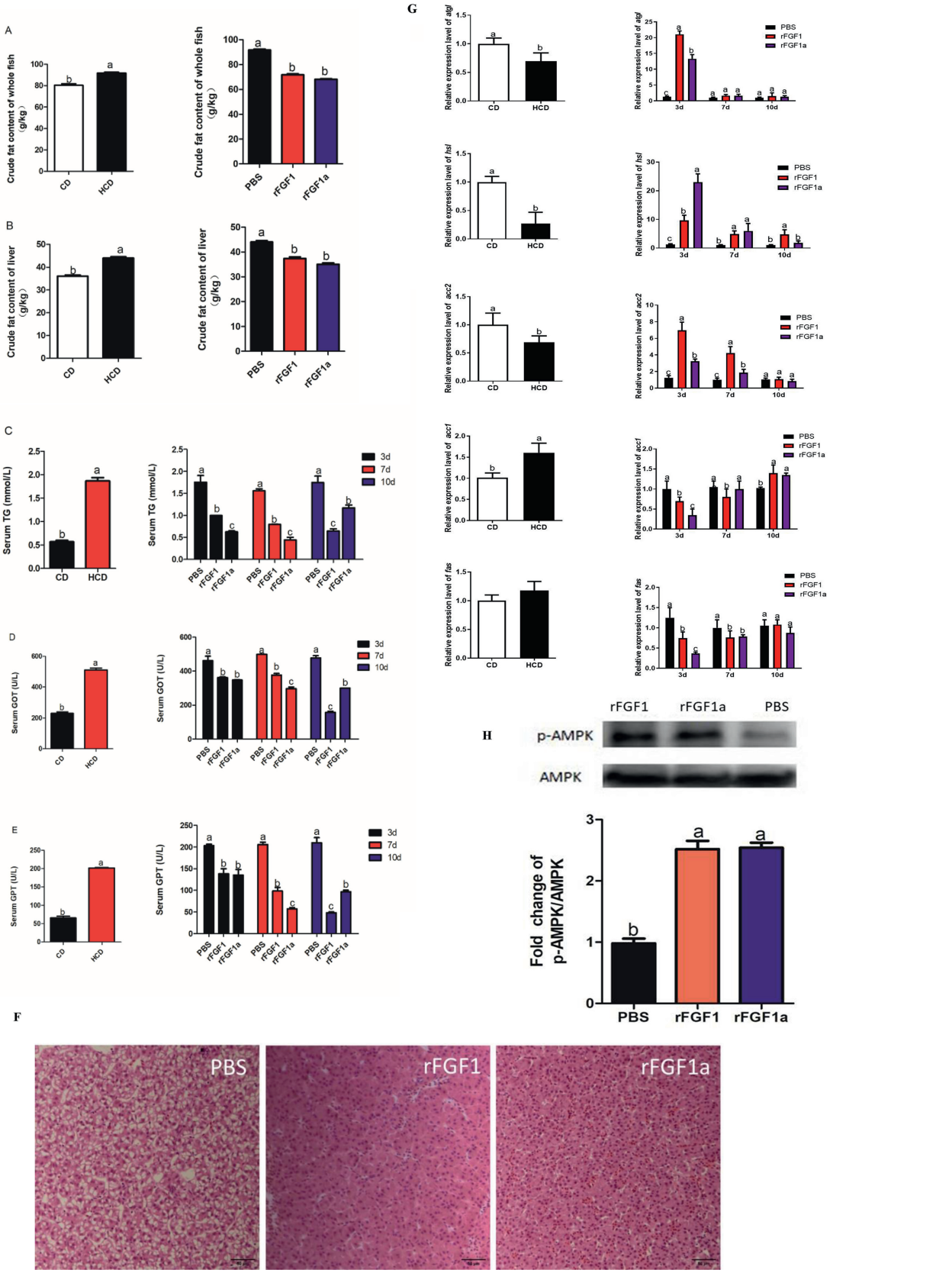

Fig. 4. Effect of different treatments on lipid metabolism in rainbow trout. (A) Whole-fish crude fat ($n = 6$). (B) Liver crude fat ($n = 6$). (C) Serum TG ($n = 6$), (D) Serum GOT ($n = 6$). (E) Serum GPT ($n = 6$). (F) Liver H&E staining ($n = 3$). (G) The mRNA expression of adipogenic and lipolytic related genes in the liver ($n = 6$). (H) Protein expression of AMPK and p-AMPK were assessed by Western blotting ($n = 3$). TG = triglyceride; GOT = glutamic oxaloacetic transaminase; GPT = glutamic pyruvic transaminase; *fas* = fatty acid synthase; *hsl* = hormone-sensitive lipase; *atgl* = adipose triglyceride lipase; *acc* = acetyl-CoA carboxylase; AMPK = adenosine monophosphate (AMP)-activated protein kinase. CD = chow diet; HCD = high-carbohydrate diet. PBS refers to the HCD group were injected with phosphate buffer saline; rFGF1 refers to the HCD group was injected with recombinant protein fibroblast growth factor 1; rFGF1a refers to the HCD group was injected with recombinant protein fibroblast growth factor 1a. $^{a-c}$ Different letters indicate significant differences between groups ($P < 0.05$).

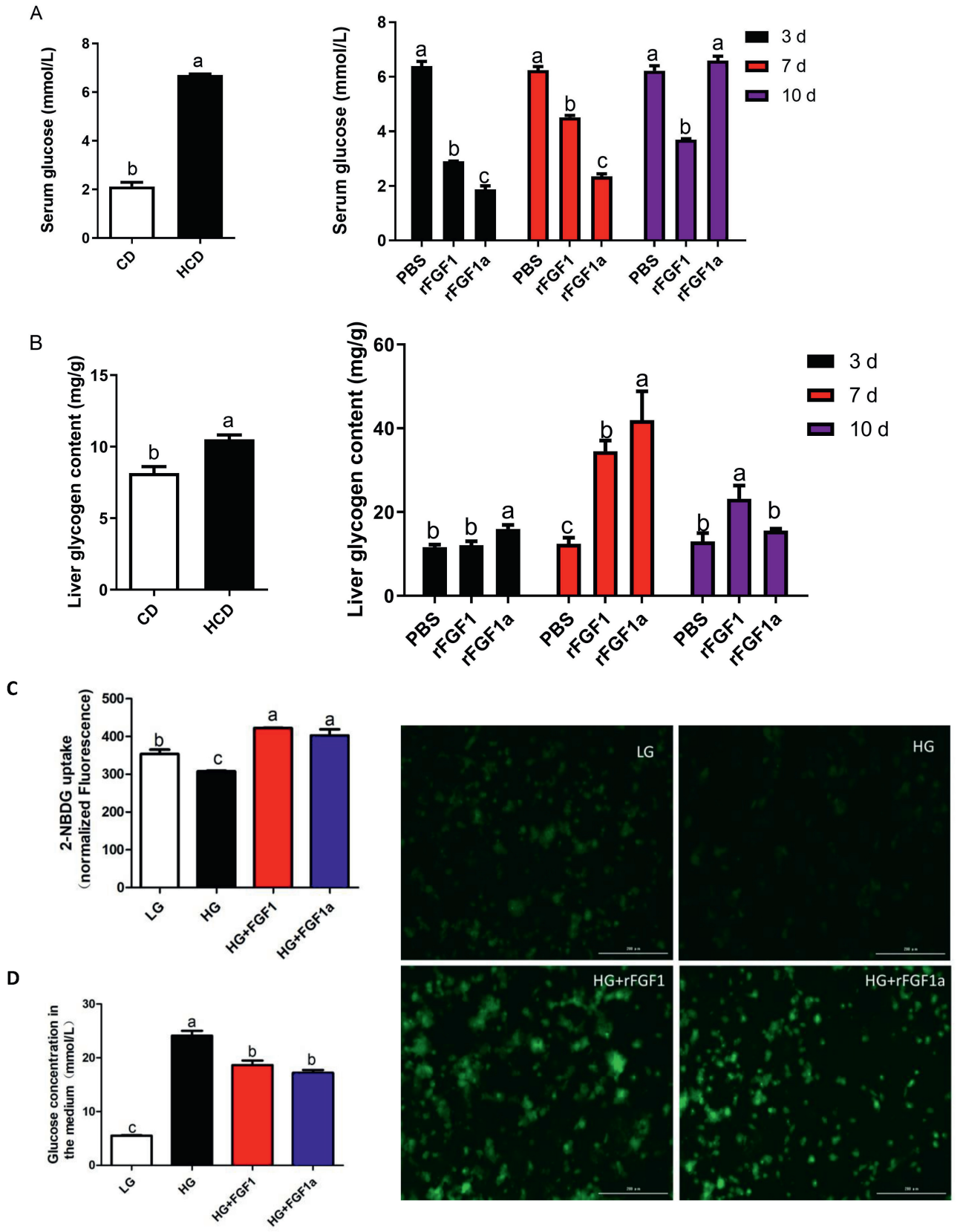

Fig. 5. Effect of different treatments on glucose utilization in rainbow trout. (A) Serum glucose ($n = 9$). (B) Hepatic glycogen ($n = 6$). (C) Glucose uptake by hepatocytes (scale bar = 200 μm; $n = 6$). (D) Glucose concentration in the medium ($n = 6$). CD = chow diet; HCD = high-carbohydrate diet. PBS refers to the HCD group injected with phosphate buffer saline; rFGF1 refers to the HCD group injected with recombinant protein fibroblast growth factor 1; rFGF1a refers to the HCD group injected with recombinant protein fibroblast growth factor 1a. LG refers to low glucose (1 g/L); HG refers to high glucose (4.5 g/L); HG + rFGF1 refers to high glucose (4.5 g/L) + recombinant protein fibroblast growth factor 1 (50 ng/μL); HG + rFGF1a refers to high glucose (4.5 g/L) + recombinant protein fibroblast growth factor 1a (50 ng/μL). Statistical differences in mean values of all indicators were assessed using independent *t*-tests. $^{a-c}$ Different letters indicate significant differences between groups ($P < 0.05$).

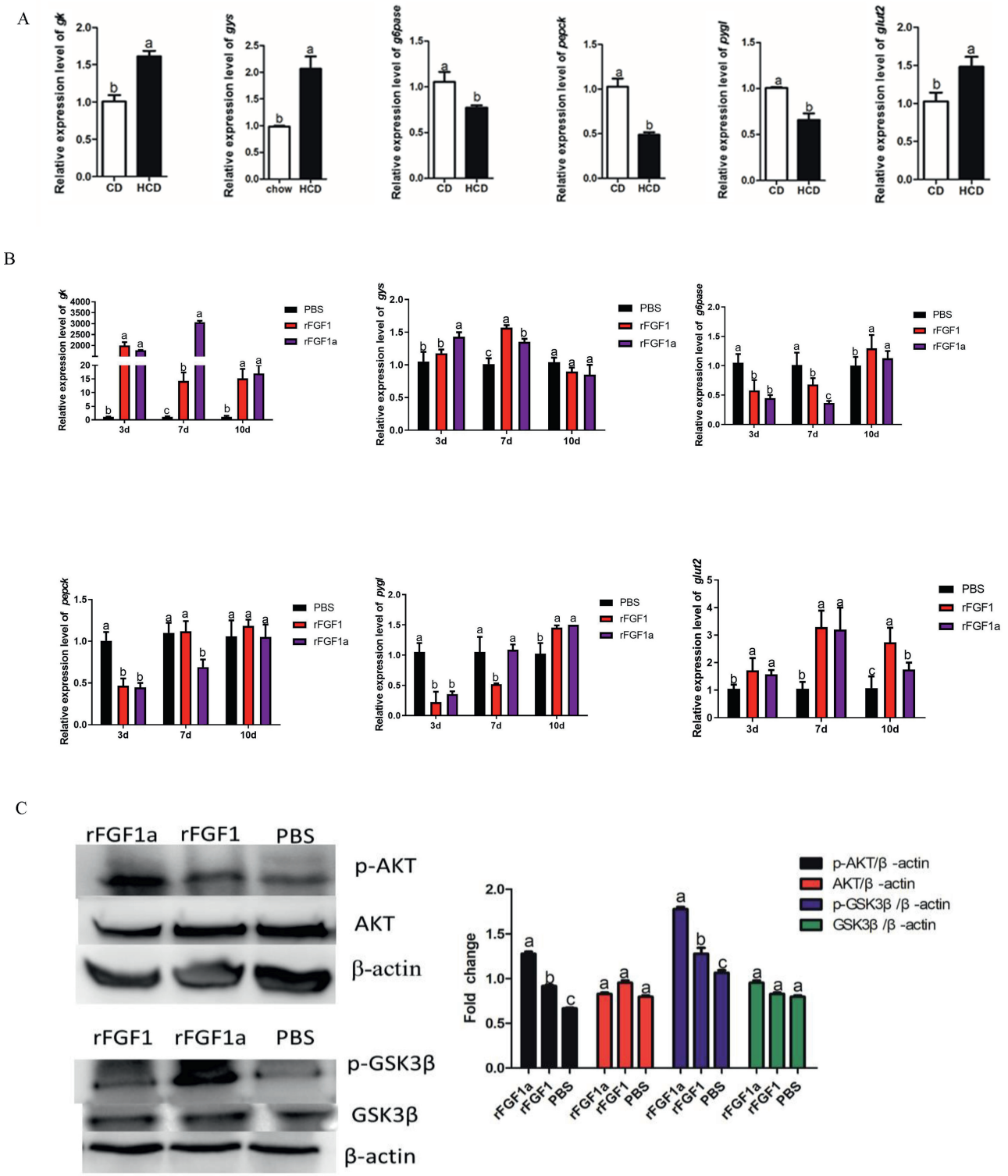

Fig. 6. Effects of different treatments on AKT/GSK3β axis and glucose metabolism-related gene expression in rainbow trout. (A) The mRNA expression of genes related to glucose metabolism by different carbohydrate content diets ($n = 9$). (B) The mRNA expression of glucose metabolism-related genes at different times after FGF1 and FGF1a treatments ($n = 9$). (C) Protein expression of AKT and GSK-3β was assessed by Western blotting ($n = 3$). *gk* = glucose kinase; *pepck* = phosphoenolpyruvate carboxykinase; *g6pase* = glucose-6-phosphatase; *pygl* = glycogen phosphorylase; *gys* = glycogen synthase; *glut2* = glucose transporter 2; CD = chow diet; HCD = high-carbohydrate diet. PBS refers to the HCD group injected with phosphate buffer saline; rFGF1 refers to the HCD group injected with recombinant protein fibroblast growth factor 1; rFGF1a refers to the HCD group injected with recombinant protein fibroblast growth factor 1a. Statistical differences in means were assessed by using a one-way analysis of variance (ANOVA) followed by independent *t*-tests. [a–c] Different letters indicate significant differences ($P < 0.05$).

expression was significantly increased in rFGF1 and rFGF1a compared with the PBS-injected group (Fig. 6B). In addition, the HCD downregulated the abundance of gluconeogenesis-related genes, *pepck* and *g6pase* compared to the CD group (Fig. 6A). Based on the HCD, rFGF1 and rFGF1a showed significant inhibition of gluconeogenesis 3 d after injection. However, this inhibition diminished with increasing time (Fig. 6B). Moreover, HCD lowered *pygl* and increased *gys* expression, and rFGF1 and rFGF1a injection groups exacerbated their changes.

To explore the molecular mechanism of hepatic glycogen changes, we further investigated the changes in AKT/GSK3β signaling pathway under intraperitoneal administration (Fig. 6C). The rFGF1 and rFGF1a injections enhanced the level of phosphorylation of AKT at position 473 in comparison to the PBS-injected group, but they had no discernible effect on the total level of AKT ($P > 0.05$). Both rFGF1 and rFGF1a dramatically enhanced the phosphorylation level of GSK3β at the Ser9 site ($P < 0.05$), but they had little effect on the protein's overall content ($P > 0.05$).

4. Discussion

In this study, we successfully cloned and characterized the *fgf1* gene in rainbow trout, which has a prototype (*fgf1*) and only one isoform (*fgf1a*) like most teleosts. This is quite different from carp. Grass carp (Guo et al., 2017), zebrafish (Songhet et al., 2007), and common carp (Ma et al., 2014) have two duplicate *fgf1s*, *fgf1a* and *fgf1b* and their production is considered additional genomic replication events (Taylor et al., 2003). The FGF1 and FGF1a polypeptides of mature rainbow trout contain a conserved FGF structural domain, indicating that both genes have been conserved throughout vertebrate evolution. Despite a lower sequence identity of 59.8%, rainbow trout FGF1 and FGF1a have high homology with their salmon counterparts in the direct lineage. Furthermore, the phylogenetic tree revealed that FGF1 and FGF1a clustered with teleosts, suggesting a closer evolutionary origin.

The glucose utilization of fish is less efficient than other animals (Kamalam et al., 2017; Li et al., 2022). Fish are naturally diabetic and develop symptoms similar to humans when their serum glucose level exceeds a certain threshold. After intravenous injection of glucose solution (≥120 mg/kg body weight) in tilapia, urinary glucose excretion takes place, and the concentration of urinary glucose will increase as the concentration of injected glucose increases (Chen et al., 2018; Lin et al., 2000; Pan et al., 2023). The plasma glucose concentration in rainbow trout reached the highest level 1 h after glucose injection (Jin et al., 2014). The results of our study indicated a significant rise in serum glucose levels following glucose injection. Despite a slight decrease in glucose levels at the 6 h mark compared to 2 h, glucose levels remained elevated.

Our findings showed that the short-term high-carbohydrate feeding group had significantly higher body weight gain than the low-carbohydrate group, supported by grass carp studies (Fang et al., 2021). However, increasing HSI in the HCD group suggested hepatomegaly. Furthermore, prolonged feeding of high carbohydrates demonstrated impaired growth performance and visceral damage (Shi et al., 2022; Villasante et al., 2022; Xu et al., 2017). Interestingly, the administration of rFGF1 and rFGF1a had no significant effect on growth performance in the short term (Table 4), and we will conduct long-term feeding experiments and continuous rFGF1 treatment in subsequent research to determine their long-term effects on rainbow trout. Excessive carbohydrate consumption in fish typically increases fat synthesis and results in ectopic fat deposition, which in turn induces oxidative stress and inflammation and ultimately harms the fish's health (Xu et al., 2022; Zhao et al., 2021). In this study, rFGF1 and rFGF1a reduced the HCD-induced lipid deposition in rainbow trout. Lipolytic effects were confirmed by increased expression of lipolysis-related genes (*atgl*, *hsl*, and *acc2*) and decreased expression of *acc1* and *fas* in the liver. Then, we observed a decrease in serum glucose levels and a downregulation of *pepck* and *g6pase*, two essential genes for hepatic gluconeogenesis, suggesting that rFGF1 and rFGF1a may be responsible for inhibiting hepatic gluconeogenesis. Moreover, an increase in hepatic glycogen synthesis is necessary for rFGF1 and rFGF1a to have a hypoglycemic impact. Our findings illustrated that hepatocytes treated with rFGF1 and rFGF1a dramatically boosted hepatic glycogen content and accelerated glucose absorption. The fluctuating levels of *gys* and *pygl* served as substantiation for this. Our results found that the role of FGF1 in inhibiting hepatic gluconeogenesis is similar to what has been observed in mammals (Huang et al., 2017; Perry et al., 2015), indicating that its function is conserved across species. However, the mechanism of action of FGF1 and insulin in regulating glucose homeostasis in vivo remains debatable, and independent or synergistic effects are possible (Huang et al., 2017). Therefore, further research is required into the mechanism of action of FGF1 and insulin in scleractinian fish.

The importance of AKT signaling has been demonstrated in many organisms, supporting its conserved role in regulating cellular metabolism (Teleman, 2010; Wang et al., 2022). AKT regulation during gluconeogenesis is primarily deduced from the relationship between AKT phosphorylation (activated by threonine phosphorylation, followed by serine phosphorylation) and GSK3β activity is inhibited after phosphorylation at the Ser9 site (Ahmed et al., 2023; Lizcano and Alessi, 2002). In addition, GSK3β regulates the glycogen synthesis capacity of animals by inhibiting the activity of the glycogen synthase GS. Reportedly, GSK3β is involved in adipogenesis (Gu et al., 2019; Liu et al., 2018). In this study, rFGF1 and rFGF1a led to an increase in AKT phosphorylation leading to AKT activation, and an increase in GSK3β phosphorylation, resulting in GSK3β protein inhibition. Moreover, AMPK regulates HSL and ATGL activity (Fang et al., 2022). Our results suggested that rFGF1 and rFGF1a significantly upregulated the AMPK signaling pathway, suggesting their regulatory role in lipid metabolism.

However, there were certain limitations to this study. In exploring the potential mechanism of the hypoglycemic ability of rFGF1 and rFGF1a, we demonstrated that rFGF1 plays its role via the AKT/GSK3β signaling pathway; nonetheless, this pathway is also one of the pathways through which insulin acts. The extent to which FGF1 acts through insulin sensitization or by differentiation from the insulin pathway is not fully understood and will be further explored in subsequent experiments.

5. Conclusion

In brief, exogenous administration of FGF1 enhanced the liver's ability to synthesize glycogen and enhanced lipolysis, and this may lead to the reduction of serum glucose and TG levels in rainbow trout. The potential mechanisms are summarized in Fig. 7. This study provides a new approach for the regulatory role of FGF1 in glycolipid utilization and homeostatic remodeling of glycolipid metabolism in carnivorous fish through the AKT/GSK3β and AMPK signaling pathways.

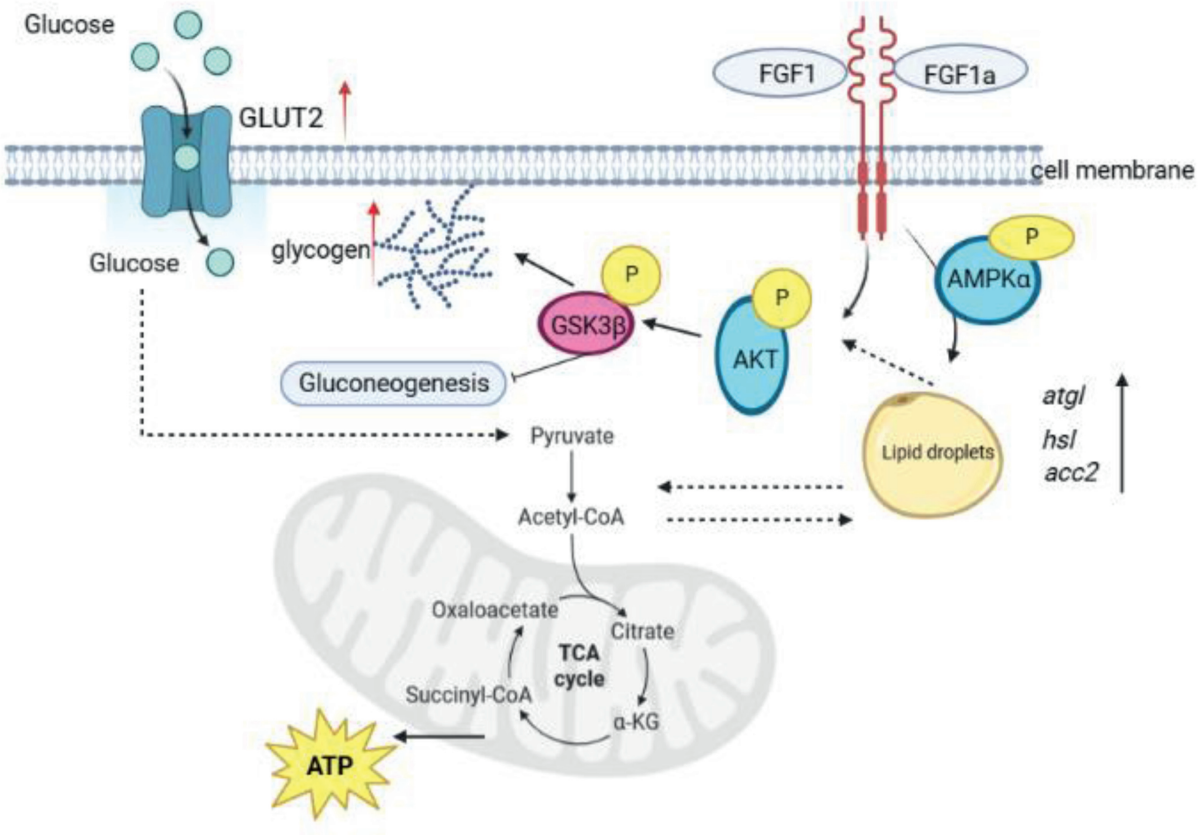

Fig. 7. Summary of the results showing rainbow trout FGF1 and FGF1a improved lipid metabolism disorders in juvenile rainbow trout, reduced hepatic and systemic lipid accumulation, inhibited gluconeogenesis and increased hepatic glycogen synthesis by regulating the AMPK pathway and AKT/GSK3β axis in rainbow trout. FGF = fibroblast growth factor; *hsl* = hormone-sensitive lipase; *atgl* = adipose triglyceride lipase; *acc* = acetyl-CoA carboxylase; GLUT2 = glucose transporter 2; AKT = serine/threonine kinase; GSK3β = glycogen synthase kinase 3β; AMPK = adenosine monophosphate (AMP)-activated protein kinase; TCA = tricarboxylic acids. This figure was created by BioRender.com (BioRender, Toronto, ON, Canada).

Author contributions

Huixia Yu: dedicated to investigation, data curation and manuscript writing. **Yang Li** and **Lixin Wang:** revised the manuscript. **Shuo Geng** and **Debin Zhong:** dedicated to part of the feeding experiment. **Xin Ren:** provided the site and rainbow trout for this study. **Haolin Mo** and **Mingxing Yao:** analyzed and interpreted the data. **Shuai Li** and **Yingwei Wang:** conducted the total RNA extraction and real-time PCR. **JiaJia Yu**, **Yang Li** and **Lixin Wang:** provided experimental guidance. All authors read and approved the final version of the manuscript.

Declaration of competing interest

We declare that we have no financial and personal relationships with other people or organizations that can inappropriately influence our work, and there is no professional or other personal interest of any nature or kind in any product, service and/or company that could be construed as influencing the content of this paper.

Acknowledgment

This research was supported by the National Natural Science Foundation of China (No. 31502180), Shaanxi Provincial Agricultural Products Quality and Safety Project (K3370220036), the National Key R & D Program of China (2019YFD0900200).

Appendix Supplementary data

Supplementary data to this article can be found online at https://doi.org/10.1016/j.aninu.2023.10.009.

References

Ahmed SA, Sarma P, Barge SR, Swargiary D, Devi GS, Borah JC. Xanthosine, a purine glycoside mediates hepatic glucose homeostasis through inhibition of gluconeogenesis and activation of glycogenesis via regulating the AMPK/FoxO1/AKT/GSK3β signaling cascade. Chem Biol Interact 2023;371:110347. https://doi.org/10.1016/j.cbi.2023.110347.

AOAC. Official Methods of Analysis of AOAC International. 18th ed. Gaithersburg, MD: AOAC International; 2005.

Chen YJ, Wang XY, Pi RR, Feng JY, Luo L, Lin SM, Wang DS. Preproinsulin expression, insulin release, and hepatic glucose metabolism after a glucose load in the omnivorous GIFT tilapia *Oreochromis niloticus*. Aquaculture 2018;482:183–92. https://doi.org/10.1016/j.aquaculture.2017.10.001.

Choi Y, Jang S, Choi MS, Ryoo ZY, Park T. Increased expression of FGF1-mediated signaling molecules in adipose tissue of obese mice. J Physiol Biochem 2016;72:157–67. https://doi.org/10.1007/s13105-016-0468-6.

Fang C, Pan J, Qu N, Lei Y, Han J, Zhang J, Han D. The AMPK pathway in fatty liver disease. Front Physiol 2022;13. https://doi.org/10.3389/fphys.2022.970292.

Fang L, Guo X, Liang XF. First feeding of grass carp (*Ctenopharyngodon idellus*) with a high-carbohydrate diet: the effect on glucose metabolism in juveniles. Aquacult Rep 2021;21:100830. https://doi.org/10.1016/j.aqrep.2021.100830.

Fujisawa K, Takami T, Okubo S, et al. Establishment of an adult medaka fatty liver model by administration of a gubra-amylin-nonalcoholic steatohepatitis diet containing high levels of palmitic acid and fructose. Int J Mol Sci 2021;22(18):9931. https://doi.org/10.3390/ijms22189931.

Gasser E, Moutos CP, Downes M, Evans RM. FGF1—a new weapon to control type 2 diabetes mellitus. Nat Rev Endocrinol 2017;13(10):599–609. https://doi.org/10.1038/nrendo.2017.78.

Gasser E, Sancar G, Downes M, Evans RM. Metabolic Messengers: fibroblast growth factor 1. Nat Metab 2022;4(6):663–71. https://doi.org/10.1038/s42255-022-00580-2.
Gu Y, Gao L, Han Q, Li A, Yu H, Liu D, Pang Q. GSK-3β at the crossroads in regulating protein synthesis and lipid deposition in Zebrafish. Cells 2019;8(3):205. https://doi.org/10.3390/cells8030205.
Guo DD, Guan WZ, Sun YW, Chen J, Jiang XY, Zou SM. Comparative expression and regulation of duplicated fibroblast growth factor 1 genes in grass carp (*Ctenopharyngodon idella*). Gen Comp Endocrinol 2017;240:61–8. https://doi.org/10.1016/j.ygcen.2016.09.014.
Huang Z, Tan Y, Gu J, Liu Y, Song L, Niu J, Mohammadi M. Uncoupling the mitogenic and metabolic functions of FGF1 by tuning FGF1-FGF receptor dimer stability. Cell Rep 2017;20(7):1717–28. https://doi.org/10.1016/j.celrep.2017.06.063.
Jin J, Médale F, Kamalam BS, Aguirre P, Véron V, Panserat S. Comparison of glucose and lipid metabolic gene expressions between fat and lean lines of rainbow trout after a glucose load. PLoS One 2014;9(8):e105548. https://doi.org/10.1371/journal.pone.0105548.
Jonker JW, Suh JM, Atkins AR, Ahmadian M, Li P, Whyte J, Evans RM. A PPARγ–FGF1 axis is required for adaptive adipose remodelling and metabolic homeostasis. Nature 2012;485(7398):391–4. https://doi.org/10.1038/nature10998.
Kamalam BS, Medale F, Panserat S. Utilisation of dietary carbohydrates in farmed fishes: new insights on influencing factors, biological limitations and future strategies. Aquaculture 2017;467:3–27. https://doi.org/10.1016/j.aquaculture.2016.02.007.
Liu D, Yu H, Pang Q, Zhang X. Investigation of the lipid-lowering effect of Vitamine C through GSK-3β/β-catenin signaling in zebrafish. Front Physiol 2018;9:1023. https://doi.org/10.3389/fphys.2018.01023.
Liu W, Struik D, Nies VJ, Jurdzinski A, Harkema L, de Bruin A, Jonker JW. Effective treatment of steatosis and steatohepatitis by fibroblast growth factor 1 in mouse models of nonalcoholic fatty liver disease. P Natl Acad Sci 2016;113(8):2288–93. https://doi.org/10.1073/pnas.1525093113.
Lin SC, Liou CH, Shiau SY. Renal threshold for urinary glucose excretion by tilapia in response to orally administered carbohydrates and injected glucose. Fish Physiol Biochem 2000;23:127–32. https://doi.org/10.1023/A:1007888108057.
Li X, Han T, Zheng S, Wu G. Hepatic glucose metabolism and its disorders in fish. Rec Adv Anim Nutr Metab 2022:207–36. https://doi.org/10.1007/978-3-030-85686-1_11.
Lizcano JM, Alessi DR. The insulin signalling pathway. Curr Biol 2002;12(7):R236–8. https://doi.org/10.1016/S0960-9822(02)00777-7.
Ma L, Jiang L, Wang Y, Cheng A, Qiao Z, Li H. Effect of FGF1a (fibroblast growth factor 1a) gene on mirror carp scale development (in Chinese). Genom Appl Biol 2014;33(1):82–7. https://doi.org/10.13417/j.gab.033.000082.
Pan J, Chen L, Ji Y, Huang Y, Bu X, Zhu J, Wang X. A crucial role in osmoregulation against hyperosmotic stress: carbohydrate and inositol metabolism in Nile tilapia (*Oreochromis niloticus*). Aquacult Rep 2023;28:101433. https://doi.org/10.1016/j.aqrep.2022.101433.
Perry RJ, Lee S, Ma L, Zhang D, Schlessinger J, Shulman GI. FGF1 and FGF19 reverse diabetes by suppression of the hypothalamic–pituitary–adrenal axis. Nat Commun 2015;6(1):6980. https://doi.org/10.1038/ncomms7980.
Sancar G, Liu S, Gasser E, Alvarez JG, Moutos C, Kim K, Evans RM. FGF1 and insulin control lipolysis by convergent pathways. Cell Metabol 2022;34(1):171–83. https://doi.org/10.1016/j.cmet.2021.12.004.
Scarlett JM, Muta K, Brown JM, Rojas JM, Matsen ME, Acharya NK, Schwartz MW. Peripheral mechanisms mediating the sustained antidiabetic action of FGF1 in the brain. Diabetes 2019;68(3):654–64. https://doi.org/10.2337/db18-0498.
Scarlett JM, Rojas JM, Matsen ME, Kaiyala KJ, Stefanovski D, Bergman RN, Schwartz MW. Central injection of fibroblast growth factor 1 induces sustained remission of diabetic hyperglycemia in rodents. Nat Med 2016;22(7):800–6. https://doi.org/10.1038/nm.4101.
Shi Y, Zhong L, Zhong H, Zhang J, Liu X, Peng M, Hu Y. Taurine supplements in high-carbohydrate diets increase growth performance of *Monopterus albus* by improving carbohydrate and lipid metabolism, reducing liver damage, and regulating intestinal microbiota. Aquaculture 2022;554:738150. https://doi.org/10.1016/j.aquaculture.2022.738150.
Songhet P, Adzic D, Reibe S, Rohr KB. Fgf1 is required for normal differentiation of erythrocytes in zebrafish primitive hematopoiesis. Dev Dynam: an official publication of the American Association of Anatomists 2007;236(3):633–43. https://doi.org/10.1002/dvdy.21056.
Steinberg CEW. Carbohydrates with emphasis on Glucose-'Life's little luxury'. Aquatic Animal Nutrition: Organic Macro-and Micro-Nutrients 2022:263–301. https://doi.org/10.1007/978-3-030-87227-4_13.
Taylor JS, Braasch I, Frickey T, Meyer A, Van de Peer Y. Genome duplication, a trait shared by 22000 species of ray-finned fish. Genome Res 2003;13:382–90. https://doi.org/10.1101/gr.640303.
Teleman AA. Molecular mechanisms of metabolic regulation by insulin in Drosophila. Biochem J 2010;425(1):13–26. https://doi.org/10.1042/BJ20091181.
Villasante A, Ramírez C, Rodríguez H, Dantagnan P, Hernández A, Figueroa E, Romero J. Dietary carbohydrate-to-protein ratio influences growth performance, hepatic health and dynamic of gut microbiota in atlantic salmon (*Salmo salar*). Anim Nutr 2022;10:261–79. https://doi.org/10.1016/j.aninu.2022.04.003.
Volkoff H, London S. Nutrition and reproduction in fish. Encyclopedia of reproduction 2018;2:1–6. https://doi.org/10.1016/B978-0-12-809633-8.20624-9.
Wang J, Zhang F, Yang W, Gao D, Yang L, Yu C, Zhang JS. FGF1 ameliorates obesity-associated hepatic steatosis by reversing IGFBP2 hypermethylation. Faseb J 2023;37(4):e22881. https://doi.org/10.1096/fj.202201950R.
Wang M, Zhang J, Gong N. Role of the PI3K/Akt signaling pathway in liver ischemia reperfusion injury: a narrative review. Ann Palliat Med 2022;11:806–17. https://doi.org/10.21037/apm-21-3286.
Wen C, Ma S, Tian H, Jiang W, Jia X, Zhang W, Zhang D. Evaluation of the protein-sparing effects of carbohydrates in the diet of the crayfish, *Procambarus clarkii*. Aquaculture 2022;556:738275. https://doi.org/10.1016/j.aquaculture.2022.738275.
Xu C, Liu WB, Dai YJ, Jiang GZ, Wang BK, Li XF. Long-term administration of benfotiamine benefits the glucose homeostasis of juvenile blunt snout bream *Megalobrama amblycephala* fed a high-carbohydrate diet. Aquaculture 2017;470:74–83. https://doi.org/10.1016/j.aquaculture.2016.12.025.
Xu R, Wang T, Ding FF, Zhou NN, Qiao F, Chen LQ, Zhang ML. Lactobacillus plantarum ameliorates high-carbohydrate diet-induced hepatic lipid accumulation and oxidative stress by upregulating uridine synthesis. Antioxidants 2022;11(7):1238. https://doi.org/10.3390/antiox11071238.
Xu Z, Wu Y, Wang F, Li X, Wang P, Li Y, Liu Y. Fibroblast growth factor 1 ameliorates diabetes-induced liver injury by reducing cellular stress and restoring autophagy. Front Pharmacol 2020;11:52. https://doi.org/10.3389/fphar.2020.00052.
Yu K, Huang K, Tang Z, Huang X, Sun L, Pang L. Metabolism and antioxidation regulation of total flavanones from Sedum sarmentosum Bunge against high-fat diet-induced fatty liver disease in Nile tilapia (*Oreochromis niloticus*). Fish Physiol Biochem 2021;47:1149–64. https://doi.org/10.1007/s10695-021-00964-3.
Zhao L, Liang J, Chen F, Tang X, Liao L, Liu Q, Rahimnejad S. High carbohydrate diet induced endoplasmic reticulum stress and oxidative stress, promoted inflammation and apoptosis, impaired intestinal barrier of juvenile largemouth bass (*Micropterus salmoides*). Fish Shellfish Immunol 2021;119:308–17. https://doi.org/10.1016/j.fsi.2021.10.019.